Bioactive Constituents, Metabolites, and Functions

Discovery of Neolignan Glycosides with Acetylcolinesterase Inhibitory Activity from Huangjinya Green Tea Guided by UPLC-MS2 data and GNPS Molecular Networking

Hao-Yue Wu, Jia-Ping Ke, Wei Wang, Ya-Shuai Kong, Peng Zhang, Tie-Jun Ling, and Guan-Hu Bao

J. Agric. Food Chem., **Just Accepted Manuscript** • DOI: 10.1021/acs.jafc.9b05605 • Publication Date (Web): 08 Oct 2019

Discovery of Neolignan Glycosides with Acetylcolinesterase Inhibitory Activity from Huangjinya Green Tea Guided by UPLC-MS^2 data and GNPS Molecular Networking

Hao-Yue **Wu**,† Jia-Ping **Ke**,† Wei **Wang**,† Ya-Shuai **Kong**,† Peng **Zhang**,† Tie-Jun **Ling**,† Guan-Hu **Bao**†,*

Natural Products Laboratory, State Key Laboratory of Tea Plant Biology and Utilization, Anhui Agricultural University, Hefei, Anhui Province 230036, China

*Corresponding author. Phone: +86-551-65786401. Fax: +86-551-65786765; E-mail: baoguanhu@ahau.edu.cn (G.-H. **Bao**).

Abstract: Global Natural Product Social (GNPS) feature based networking was applied to follow the phytochemicals including 9 flavonoid glycosides, 6 catechins, and 3 flavonols in Huangjinya green tea. Further, a new 8-*O*-4′-type neolignan glycoside, camellignanoside A (**1**), together with 15 known compounds (**2**-**16**), were isolated through a variety of column chromatography, and the structure was elucidated extensively by UPLC-Q-TOF-MS^2, ^1H and ^{13}C NMR, HSQC, HMBC, ^1H-^1H CCOY, ROESY, and NOESY, and circular dichroism (CD) spectroscopies. Compounds **1** and **2** showed acetylcolinesterase (AChE) inhibition activity with IC_{50} = 0.75 and 0.18 μM, respectively.

Keywords: Huangjinya, green tea, *Camellia sinensis*, neolignan glycosides, GNPS, Acetylcholinesterase

INTRODUCTION

Tea, made of leaf or bud plucked from the plant *Camellia sinensis*, is popularly consumed all round the world. It is classified into six major types as green, yellow, white, oolong, black, or dark tea.[1-3] Among them, green tea has been studied the most extensively because of its significant health benefits.

Huangjinya, a natural tea mutant, is one special light-sensitive albino cultivar (*Camellia sinensis* var. *sinensis* cv. Huangjinya). The tender shoots are albino under sun-light, whereas turn green with different shading conditions, which is just the opposite to the case of Anji white tea.[4,5] This albino mutant has high content of free amino acids, improving drinking quality. Previous researches focused on the characteristics and underlying formation mechanism of albino tea,[6] emphasized on the analysis of changes in transcriptome and proteome,[7] and the expression of photoreceptor genes.[8] However, purification of phytochemicals from this albino mutant has never been approached.

Here, we used GNPS to automatically analyze the phytochemicals from Huangjinya green tea extract (HGTE) based on the tandem mass (MS/MS, MS^2) data. Three major clusters including catechins, flavonoid glycosides, as well as neolignan glycosides were achieved according to the MS^2 similarity, further supervising the isolation and elucidation of phytochemicals in HGTE. One new 8-*O*-4′-type neolignan glycoside, camellignanoside A, together with 15 known compounds (**2**-**16**) were isolated and identified (**Figure 1**). Their structures were determined by analyses of their UPLC-Q-TOF-MS/MS, 1D and 2D NMR, IR and circular dichroism (CD)

spectroscopic data as well as comparison with those in literature.

Neolignans had been reported from various food-related plants including tea. They are biosynthesized through the shikimic acid pathway and possess a variety of bioactivities including antitumor,[9] antioxidant,[10] anti-inflammation,[11] antipsychotic,[12] neuroprotective,[13] and anti-acetylcholinesterase activity.[14]

Alzheimer's disease (AD) is an irreversible neurodegenerative disorder, usually associated with neuron loss in the central nervous system.[13] Discovery of agents able to inhibit the activity of acetylcholinesterase (AChE) has been reported as one effective approach to treat AD.[15] We found that tea polyphenols, especially catechins esterzied with hydroxycinnamic acid, have strong AChE inhibition activity.[15] As such, we also tested the AChE inhibitory activity of **1** and **2**, indicating that **2** showed stronger while **1** showed less inhibition against AChE than the positive AChE inhibitor huperzine A (hup A).

MATERIALS AND METHODS

Chemicals. HPLC grade of methanol (MeOH), acetonitrile (AcN), formic acid (HCOOH) (DUKSAN, Ansansi, Korea) was used for HPLC analysis and purification. Analytical grade of petroleum ether (PE), ethyl acetate (EtOAc), MeOH, dichloromethane (CH_2Cl_2), were used for extraction and isolation (Chengdu Kelong Chemical Reagent Co., Ltd, Chengdu, China). Chloroform-*d* ($CDCl_3$) and dimethyl-d_6 sulfoxide (DMSO-d_6) were bought from Cambridge Isotope Laboratories, Inc. (Andover, MA, USA). Column chromatography (CC) were performed with silica gel (Yantai Jiangyou Silicon Development Co., Ltd., Shandong, China), MCI-Gel

CHP20P (Mitsubishi Ltd., Japan), Toyopearl HW-40F (Tosoh Bioscience Shanghai Co., Ltd., Shanghai, China), Sephadex LH-20 (GE Healthcare Bio-Sciences AB, Sweden). All the flowing reagents were used in the AChE inhibitory activity assay: 5, 5'-dithiobis (2-nitrobenzoic acid) (DTNB) and acetylthiocholine iodide (ATCI) (Fluka, Shanghai, China), AChE (500 U, Type VI-S Electric Eel) (Sigma-Aldrich, Shanghai, China), hup A (Herbest, Shanxi, China) and phosphate buffer saline (PBS) (Splarbio, Beijing, China).

NMR spectra including one dimensional (^{1}H, ^{13}C NMR, and DEPT-135) and two dimensional (^{1}H-^{1}HCOSY, HSQC, HMBC, ROESY, and NOESY) were acquired in DMSO-d_6 with Agilent DD2 600 MHz. IR spectra were recorded on an FTIR-650 spectrometer purchased from GangDong Sci. & Tech. Development Co., Ltd. (Tianjin, China). The Agilent 6210 UPLC-Q-TOF-MS/MS system has a photodiode array detector (PAD), coupled to a HR-TOF-MS, with electrospray ionization (ESI) source. Optical rotations were obtained with MCP 100 modular circular polarimeter (Anton Paar GmbH, Graz, Austria). JASCO J-815 spectropolarimeter (JASCO, Tokyo, Japan) was used to measure circular dichroism spectra.

Plant Sample. Huangjinya (*Camellia sinensis* var. *sinensis* cv. Huangjinya) green tea was purchased from Anji, Zhejiang Province, China, collected in April, 2017. The tea sample was deposited at the Natural Products Laboratory of Anhui Agricultural University.

LC-MS^2 Detection for Molecular Networking. Tea sample (160 mg) was extracted with 70% MeOH (8 mL) in 10 mL glass flask volumetric by ultrasonic twice for 2 h

each time at room temperature. The extract was centrifuged at 10,000 rpm for 10 min. Took out the supernatant and filtered it with 0.22 μm syringe filters for LC-MS analysis. The tea extracts were monitored using an Agilent 6210 UPLC-Q-TOF-MS/MS. The chromatographic separation was equipped with ACQUITY UPLC BEH Shield RP18 column (2.1 × 150 mm, i.d., 1.7 μm). Column temperature was set at 25 °C. The UPLC parameters were as follows: The injection volume was 3 μL. The flow rate was 0.3 mL/min. The eluent was composed of A (water with 0.1% formic acid) and B (acetonitrile with 0.1% formic acid). The gradient elution was as follows: 90% A for 0–1, 90-85% A for 1-2.5, 85-82% A for 2.5-7, 82-90% A for 7-8, 90-84% A for 8-10, 84-82% A for 10-10.5, 82-78% A for 10.5-12, 78-77% A for 12-14, 77-5% A for 14-15, and 5% A for 15-18, 5-90% A for 18-21 min. The UV was detected with a PAD at full-length scan ranging from 190 to 400 nm.

Molecular Networking. The complete molecular networking of HGTE was created through the online workflow at GNPS platform (https://gnps.ucsd.edu/ProteoSAFe/index.jsp?task=25d18427537b4d93b8df362c533f8e2b). 0.02 Da parent mass and MS^2 fragment ion tolerance was used to cluster the data and create consensus spectra. Additionally, we discarded the consensus spectra containing less than 4 spectra in the experiments. A network with edges filtered to have a cosine score above 0.5 was then created.

Purification Procedure. Huangjinya green tea (8 kg) was ground and extracted with PE (15 L), EtOAc (15 L), and MeOH (20 L) for three times at room temperature,

successively. The tea leaves were entirely soaked by the solvent during all the extraction process. The crude extract was concentrated in vacuo and fractions A-C were got: fraction A (PE fraction, 36 g), fraction B (EtOAc fraction, 85 g), and fraction C (MeOH fraction, 1123 g). Fraction C was dissolved in water and extracted with CH_2Cl_2. The resulting water residue (800 g) was further divided into eight fractions (C1 to C8) by MCI gel CC (60 cm × 7 cm, length × internal diameter, abbreviated as 60 × 7 cm) eluted with MeOH-H_2O (0:1 to 1:0, v/v). Fraction C4 (19.6 g) was further separated with a Toyopearl CC (45 × 3.5 cm) by methanol/water (0:1 to 1:0, v/v), 1200 mL per gradient, leading to further fractions D1 to D10. Fraction D1 was applied to a LH-20 CC (60 × 1.5 cm) eluted with MeOH (500 mL) to yield E1 to E3. Compounds **1** (7 mg) and **2** (21 mg) from E1 were achieved through repeated HPLC performed on an X-Bridge Prep C18 (10 × 250 mm i.d., 5 μm) at 30 °C. The HPLC parameters were as follows: injection volume, 30 μL; flow rate, 2.0 mL/min. The mobile phase was composed of water (A) and AcN (B). The timeline gradient of A was (min, %, **Table S1**): 0–35, 87, 35-36, from 87-70, then kept at 70 for 2 min, 38-39, from 70-87%, then kept at 87% for 6 min. The UV was detected at wavelength 210 and 280 nm (**Figure S1**).

Fraction C2 was applied on LH-20 CC (50 × 3.5 cm), Toyopearl CC (60 × 3.5 cm) to yield nine fractions, F1-F9. F2 was **11** (16.5 mg), F4 was **4** (21.4 mg), F5 was **3** (28.5 mg), F6 was **5** (72.4 mg). F3 was applied on Toyopearl with MeOH to yield **8** (15.6 mg).

Fraction C3 was separated by Toyopearl CC (50 × 3.6 cm), LH-20 CC (60 × 2.5 cm)

to yield fraction G1 to G7. Fraction G4 was subject to LH-20 CC to get **6** (62.5 mg), **7** (16.3 mg). Fraction G2 was separated by silica gel CC eluted with EtOAc-MeOH (10:1 to 0:1) to yeild **10** (22.3 mg). Fraction G3 was applied on Toyopearl CC with MeOH to yield **9** (13.2 mg).

Fraction B (50 g) was divided into seven fractions B1 − B7 by a MCI CC with MeOH-H_2O (1:0 to 0:1). Fraction B5 (10.5 g) was separated by a silica gel CC eluted with CH_2Cl_2-MeOH solution with increasing polarity (50:1 to 0:1) to obtain eight fractions, H1-H8. H5 was compound **12** (243.1 mg). Compound **14** (80.5 mg) was purified from fraction B3 using Toyopearl CC. Compound **13** (175.3 mg) was isolated from fraction B4 (8 g) using silica gel CC with a mixture of CH_2Cl_2 and MeOH in a gradient elution (30:1 to 0:1) and LH-20 CC with MeOH.

Fraction D5 was applied on LH-20 CC (60 × 1.5 cm) with MeOH to give **15** (38.6 mg) and **16** (15.6 mg).

Camellignanoside A (1), UV λ_{max} (MeOH) nm 204.7, 228.2, 279.2. $[\alpha]_{25}^{D}$ = +4.5 (c 0.4, MeOH); CD (c 0.05, 70% aqueous CH_3CN, nm ($\Delta\varepsilon$)), 207 (- 4.84), 238 (+ 5.62). IR (KBr): ν_{max} 3385, 1605, 1511, and 1029 cm^{-1}. HR-ESI-MS *m/z* 539.2119 $[M-H]^-$ ($C_{26}H_{35}O_{12}$, calcd 539.2129). ^1H and ^{13}C NMR data was shown in **Table 1**.

Compound 2, UV λ_{max} (MeOH) nm, 205.8, 228.2, 279.2. $[\alpha]_{25}^{D}$ = +2.6 (c 0.08, MeOH); CD (c 0.05, 70% aqueous CH_3CN, nm ($\Delta\varepsilon$)), 211 (- 1.15), 237 (+ 11.96). IR (KBr): ν_{max} 3373, 1604, 1513, and 1077 cm^{-1}. HR-ESI-TOF *m/z* 539.2110 $[M-H]^-$ ($C_{26}H_{35}O_{12}$, calcd 539.2129). ^1H and ^{13}C NMR data was shown in **Table 1**.

Enzymatic Hydrolysis of 1 and 2. The enzymatic hydrolysis reaction was assessed

by Zhao's procedure with some modifications.[16] Briefly, at 37 °C for 24 h, about 1.8 mg of **1** and 2 mg of **2** were respectively hydrolyzed by 40 mg *β*-glucosidase in 2 mL H_2O. Then the hydrolysate was extracted three times with EtOAc. The EtOAc phases were isolated and purified to obtain aglycones **1a** and **2a**, separately. The aqueous phases were isolated and purified to give glucose. The glucose moiety was identified by GC-MS with the authentic *β*-D-glucose (**Figure S40**) using the method reported in our previous paper.[1]

Inhibition of AChE. Inhibition of AChE was conducted in accordance with the method previously used with some modifications.[15,17] The solution was composed of 160 μL of 0.001 M DTNB, 50 μL of 0.5 U mL^{-1} AChE, 20 μL of the test samples. series concentration of **1** and **2** was 0.01, 0.1, 0.5, 1, 10, 100 μM. The reaction solution was incubated at 37 °C for 20 min. Additional ATCI (20 μL, 0.0075 M) was put in the solution and incubated again for 5 min. To determine the blank value, AChE was replaced by the buffer (50 μL), the tested samples were replaced by 20 μL buffer solution. Only the test compounds solution was replaced by 20 μL buffer as the reference value. Each experimental concentration was determined trice by SpectraMax 190 microplate reader (25 °C, 412 nm). The percent inhibition was calculated by the formula:

AChE inhibitory activity (%) = (Ar - At) / (Ar - Ab) × 100 %, where Ar is absorbance of reference, At is absorbance of test and Ab is absorbance of blank. Hup A was the positive control.

Statistical Analysis. The assay experiments were conducted for at least three times,

and the results were given as mean ± standard deviation (SD). GraphPad Prism software (version 6.0) was the software for statistical analysis.

RESULTS AND DISCUSSION

Molecular Networking of Tea Polyphenols from Huangjinya Green Tea. Molecular networking of HGTE on the basis of the similarity of the MS^2 spectra was generated by GNPS, including 43 clusters (node ≥ 2) and 728 single nodes. Additional details could be referred to the GNPS platform (https://gnps.ucsd.edu/ProteoSAFe/status.jsp?task=25d18427537b4d93b8df362c533f8e2b).

The results revealed the presence of 1 neolignan and 3 distinct tea polyphenol clusters. As shown in the black frame of **Figure 2**, GNPS generated four clusters efficiently including neolignans (Cluster I), flavonoid glycosides (Cluster II), catechins (Cluster III), and flavonol aglycones (Cluster IV), which can be clearly separated from each other by the MS^2 fragments. The three flavonol aglycones were identified to be kaempferol, quercetin, and myricetin through the GNPS library (labeled as pink in **Figure S41**), which were also confirmed through later purification.

The reference compound with *m/z* 561.1914 $[M + Na]^+$, was identified to be a known neolignan but was found from tea for the first time[18] (labeled as green in **Figure 2**) through the GNPS library and the MS^2 data, suggesting that these compounds were 8-*O*-4′-type neolignans. Thus, neolignans are the major composition of Cluster I (**Figure 2**). The compound with *m/z* 563.2072 $[M + Na]^+$ was also clustered, which was further purified and elucidated as a new neolignan and the details were presented

and discussed in the next section. In addition, this phenomenon also shows that compounds with the same skeleton type are clustered together.

MS^2 of flavonoid glycosides (Cluster II), was clustered into a distinct group of nodes (**Figure 3**). With the help of the reference compounds quercetin- and kaempferol-3-*O*-rutinoside, the *m/z* 773.209, 757.214, 449.106 were tentatively identified as quercetin- and kaempferol- 3-*O*-galactosylrutinoside, kaempferol-3-*O*-glucoside (**Figure 3**).[19] Another series of ions with *m/z* 481.093, 465.103 were also clustered, which were tentatively identified as quercetin 3-*O*-galactoside, myricetin 3-*O*-glucoside.

To study the structure of the phytochemicals in the cluster III, four catechins including epicatechin (EC), epicatechin 3-*O*-gallate (ECG), epigallocatechin 3-*O*-gallate (EGCG), epiafzelechin 3-*O*-gallate (EAG) were used as references for GNPS analysis (**Figure 2**). The ions of *m/z* 307.081 and 473.105 corresponded to epigallocatechin (EGC) and epigallocatechin 3-*O*-gallate-4″-methyl (EGCG4″Me).

Separation and Purification of 1-16. Huangjinya tea sample was grounded and extracted with PE, EtOAc and MeOH for three times, successively. The MeOH fraction (fraction C) was separated by opened CC, then further by semipreparative HPLC (**Figure S1**) to give a new neolignan glycoside (**1**).

Compound **1** was got as a colourless powder, with the $[M-H]^-$ signal at *m/z* 539.2119 ($C_{26}H_{35}O_{12}$, calcd 539.2129) in negative mode, suggesting that it has a molecular formula $C_{26}H_{36}O_{12}$, with 9 degrees of unsaturation. Firstly, ^1H NMR (600 MHz, DMSO-d_6) combined with ^1H-^1H COSY and HSQC spectra (**Table 1**) showed

two sets of ABX aromatic ring signals, δ_H 6.99 (s), 6.95 (d, J = 7.8 Hz), 6.78 (d, J = 7.8 Hz), and δ_H 6.73 (s), 6.66 (d, J = 7.8 Hz), 6.62 (d, J = 7.8 Hz). **1** aslo has trimethylene protons [δ_H 1.67 (2H, m), 2.48 (2H, t, J = 1.8 Hz), 3.37 (2H, t, J = 5.4 Hz)], two methoxyl group protons [δ_H 3.68 (3H, s), 3.72 (3H, s)], two methine protons [δ_H 4.76 (1H, d, J = 4.2 Hz), 4.42 (1H, m)], a β-D-glucopyranosyl anomeric proton [δ_H 4.08 (1H, d, J = 7.8 Hz)]. The presence of two C6-C3 units arising from neolignan and a β-D-glucopyranoside moiety was suggested according to the ^{13}C NMR spectrum (**Table 1**). The HMBC correlations between glucopyranosyl H-1″ and C-9, C-1″ and H-9 suggested that the β-D-glucopyranoside was attached at postion 9-OH. More HMBC correlations (**Figure 4**) from H-8′ to C-1′, H-6′ to C-7′, H-8 to C-4′, H-8 to C-1, H-9 to C-7, H-7 to C-9, H-7 to C-2, further suggested that **1** is a 8-*O*-4′-neolignan 9-*O*-glucoside.

A large and small J value for H-7 and H-8 of 8-*O*-4′-neolignan diastereoisomers correspond to the *threo* (around 7 Hz) and *erythro* (around 4 Hz) form, respectively.[20] Hydrolysis of **1** with β-glucosidase produced **1a** and D-glucose. $J_{H\text{-}7,8}$ value of **1a** is 3.6 Hz, implying that **1** could be determined to have relative *erythro*-configuration.[21]

The further CD and ROESY spectroscopic evidences could establish its absolute configurations at C-7 and C-8. The positive Cotton effect (+5.62) at 238 nm indicated that **1** has an 8*S* configuration (**Figure S33**).[22] Clear ROESY correlation between H-7 and H-8, H-8 and H-5′ as shown in **Figure 4**, suggesting the H-7 has the same β-orientation as that of H-8. Consequently, the structure of **1** was considered to be as shown in **Figure 4** with 7*R*, 8*S*-configuration.

Compound **2** is an amorphous powder, with the same molecular formula, $C_{26}H_{36}O_{12}$, as that of **1**, its $[M-H]^-$ signal at *m/z* 539.2110 ($C_{26}H_{35}O_{12}$, calcd 539.2129) in negative mode, with 9 degrees of unsaturation. The NMR data of compound **2** is very similar to those of **1** (**Table 1**). The only difference is that the glucose group is connected at position 7-OH for compound **2**, which can be confirmed by the HMBC correlations between H-1″ and C-7, C-1″ and H-7. Hydrolysis of **2** with *β*-glucosidase produced **2a** and D-glucose. The large $J_{H-7,8}$ value (8.4 Hz) (**Table 1**) of the aglycone (**2a**) and a positive Cotton effect near 237 nm suggested that the absolute configurations at C-7 and C-8 of **2** could be established as 7*S*, 8*S*.[21]

From above evidence, compounds **1** and **2** were identified as (+) -(7*R*,8*S*)-*erythro*-4,7,9′-trihydroxy-8-*O*-4′-neolignan-9-*O*-*β*-D-glucopyranoside and (7*S*,8*S*)-*threo*-4,9,9′-trihydroxy-8-*O*-4′-neolignan-7-*O*-*β*-D-glucopyranoside.

The other compounds were confirmed as EC (**3**), EGC (**4**), ECG (**5**), EGCG (**6**), EAG (**7**), epicatechin-3-*O*-gallate-3″-methyl (**8**), epigallocatechin 3-*O*-gallate-3″-methyl (**9**), gallate (**10**), methyl gallate (**11**), kaempferol (**12**), quercetin (**13**), myricetin (**14**), kaempferol 3-*O*-rutinoside (**15**), and quercetin 3-*O*-rutinoside (**16**).

AChE Inhibitory Assay. Compound **2** showed significant inhibition activity with IC_{50} value at 0.18 μM, compared with the positive control hup A (IC_{50} = 0.29 μM). **1** also showed strong activity (IC_{50} = 0.75 μM).

We have studied the chemical constituents from green,[2,23,24] white,[25] and black tea,[26] while paid little attention to albino tea mutants. Under certain environment, leaves of

256 the albino tea cultivars become bleaching and their amino acid contents increase
257 obviously compared to common green leaves. However, studies on the chemical
258 constituents are seldom reported. Here, we first used GNPS to guide the isolation and
259 identification of compounds from HGTE. GNPS is a recent published Molecular
260 networking, which is developed as the world's largest repository and data analysis
261 tool for MS^2 data.[27] Assisted by GNPS, we can systematically compared and
262 categorize large numbers of chemicals according to the structural similarities, high
263 throughput dereplicating natural products. Nowadays, GNPS is becoming an efficient
264 tool to trace natural products for purification or metabolomic purpose. In 2017, Ge et
265 al. extracted triterpenoid saponins from *Eleutherococcus senticosus* leaves (ESL),
266 using MS^2 data networking for rapid tracking 106 triterpene saponins.[28] In this paper,
267 with the help of GNPS, three major clusters including neolignan glycosides, flavonoid
268 glycosides and catechins were achieved according to the MS^2 similarity, leading to
269 speedy discovery and structural elucidation of phtochemicals in HGTE for the first
270 time. Recently, phenylpropanoidated catechins,[2] flavonol glycosides,[1,23]
271 flavoalkaloids,[24,25] and dimeric alkaloids,[3,26] have been reported from different kinds
272 of tea, however, neolignan glycosides have seldom been discovered from tea.
273 A growing body of evidence continues to emerge, demonstrating a variety of potential
274 health benefits of neolignans. In 2018, Şöhretoğlu et al. tested AChE, tyrosinase,
275 *α*-glucosidase, and butyrylcholinesterase (BuChE) inhibitory effects of
276 (-)-4-*O*-methyldehydrodiconiferyl alcohol 9'-*O*-*β*-glucopyranoside, which suggested
277 that it had good tyrosinase inhibition, however, very little inhibition against AChE,

BuChE, and α-glucosidase.[29] Kantham et al. reported that honokiol, a biphenyl neolignan, showed moderate-to-weak cholinesterases inhibition. Further, honokiol shared higher stability than EGCG.[13] Zhao et al. isolated five pairs of 8-*O*-4′ neolignans from the fruit of *Crataequs pinnatifida* Bge, most of which exhitited noticeable neuroprotective acitvity against H_2O_2-induced damage in SH-SY5Y cells.[30] Sun *et al*. isolated a new neolignan glycoside from the roots of *Spiraea salicifolia* L., which showed significant anti-inflammatory effects.[31] As such, the neolignans may also contribute to the health benefits of tea.

In summary, we reported the purification and structural elucidation of a new 8-*O*-4′-type neolignan glycoside, camellignanoside A, together with 15 known compounds (**2-16**) from Huangjinya green tea guided by GNPS. The considerable AChE inhibition of **1** and **2** suggested that this special tea albino mutant may be potentially developed as potential agent for treatment of AD or related neurodegenerative disorder.

ASSOCIATED CONTENT

Supporting Information

The Supporting data is available free of charge on the ACS Publications website at DOI:

HPLC preparation method (**Table S1**), AChE inhibitory assay result (**Table S2**), HPLC purity detection (**Figure S1-2**), UV spectra of **1** and **2** (**Figure S3-4**), NMR spectra of **1** and **2** (**Figure S5-16**), HR-ESI-MS spectrum of **1-16** (**Figure S17-32**), CD spectra of **1** and **2** (**Figure S33-34**), purity checks of **1** and **2** by HPLC with a

chiral column (**Figure S35**), ^{1}H NMR data of **1a** and **2a (Figure S36-37)**, IR spectra of **1** and **2** (**Figure S38-39**), GC-MS identification of the glucose (Glc) moiety of **1** (**Figure S40**), Molecular networking of flavonols (**Figure S41**).

AUTHOR INFORMATION

ORCID

Guan-Hu Bao: 0000-0003-4336-5678

Acknowledgements and Funding

This paper was supported by the grant from National Natural Science Foundation of China 31972462, and Anhui Provincial Key Research and Development Plan 201904a06020011.

REFERENCES

(1) Bai, W. X.; Wang, C.; Wang, Y. J.; Zheng, W. J.; Wang, W.; Wan, X. C.; Bao, G. H. Novel acylated flavonol tetraglycoside with inhibitory effect on lipid accumulation in 3T3-L1 cells from Lu'an GuaPian tea and quantification of flavonoid glycosides in six major processing types of tea. *J. Agric. Food Chem.* **2017**, *65*, 2999-3005.

(2) Ke, J. P.; Dai, W. T; Zheng, W. J.; Wu, H. Y.; Hua, F.; Hu, F. L.; Chu, G. X.; Bao, G. H. Two pairs of isomerically new phenylpropanoidated epicatechin gallates with neuroprotective effects on H_2O_2-injured SH-SY5Y Cells from Zijuan green tea and their changes in fresh tea leaves collected from different months and final product. *J. Agric. Food Chem.* **2019**, *67*, 4831-4838.

(3) Wang, W.; Tang, X.; Hua, F.; Ling, T. J.; Wan, X. C.; Bao, G.H. Camellimidazole A−C, three methylene-bridged dimeric imidazole alkaloids from Keemun black tea.

322 *Org. Lett*. **2018**, *20*, 2672-2675.

323 (4) Song, L. B.; Ma, Q. P.; Zou, Z. W.; Sun, K.; Yao, Y. T.; Tao, J. H.; Kaleri, N. A.;

324 Li, X. H. Molecular Link between Leaf Coloration and Gene Expression of Flavonoid

325 and Carotenoid Biosynthesis in Camellia sinensis Cultivar 'Huangjinya'. *Front. Plant*

326 *Sci*. **2017**, *8*, 803.

327 (5) Feng, L.; Gao, M. J.; Hou, R. Y.; Hu, X. Y.; Zhang, L.; Wan, X. C.; Wei, S.

328 Determination of quality constituents in the young leaves of albino tea cultivars.

329 *Food. Chem*. **2014**, *155*, 98-104.

330 (6) Fan, Y. G.; Zhao, X. X.; Wang, H. Y.; Tian, Y. Y.; Xiang, Q. Z.; Zhang, L. X.

331 Effect of light intensity on metabolism of light-harvesting pigment and photosynthetic

332 system in *Camellia sinensis* L. cultivar 'Huangjinya'. *Environ. Exp. Bot*. **2019**, DOI:

333 https://doi.org/10.1016/j.envexpbot.2019.06.009

334 (7) Zhang, Q. F.; Liu, M. Y.; Ruan, J. Y. Integrated transcriptome and metabolic

335 analyses reveals novel insights into free amino acid metabolism in Huangjinya tea

336 cultivar. *Front. Plant Sci.* **2017**, *8*, 291.

337 (8) Tian, Y. Y.; Wang, H. Y.; Sun, P.; Fan, Y. G.; Qiao, M. M.; Zhang, L. X.; Zhang,

338 Z. Q. Response of leaf color and the expression of photoreceptor genes of *Camellia*

339 *sinensis* cv. Huangjinya to different light quality conditions. *Sci. Hortic.* **2019**, *215*,

340 225-232.

341 (9) Xu, L. J.; Huang, F.; Chen, S. B.; Li, L. N.; Chen, S. L.; Xiao, P. G. A cytotoxic

342 neolignan from Schisandrapropinqua (Wall.) Baill. *J. Integr. Plant Biol.* **2006**, *48(12)*,

343 1493-1497.

(10) Jaidee, W.; Maneerat, W.; Andersen, R. J.; Patrick, B. O.; Pyne, S. G.; Laphookhieo, S. Antioxidant neolignans from the twigs and leaves of Mitrephora wangii HU. *Fitoterapia*. **2018**, *130*, 219-224.

(11) Salleh, W. M. N. H. W.; Ahmad, F.; Yen, K. H.; Zulkifli, R. M.; Sarker, S. D. Madangones A and B: Two new neolignans from the stem bark of Beilschmiedia madang and their bioactivities. *Phytochem. Lett.* **2016**, *15*, 168-173.

(12) Son, Y. K.; Lee, M. H.; Han, Y. N. A new antipsychotic effective neolignan from Firmiana simplex. *Arch. Pharm. Res*. **2005**, *28*, 34-38.

(13) Kantham, S.; Chan, S.; McColl, G.; Miles, J. A.; Veliyath, S. K.; Deora, G. S.; Dighe, S. N.; Khabbazi, S.; Parat, M. O.; Ross, B. P. Effect of the biphenyl neolignan honokiol on Aβ_{42}-induced toxicity in *Caenorhabditis elegans*, Aβ_{42} ibrillation, cholinesterase activity, DPPH radicals, and iron(II) chelation. *ACS Chem. Neurosci*. **2017**, *8*, 1901-1912.

(14) Dong, C. F.; Liu, L.; Luo, H. R.; Li, X. N.; Guan, Z. Y.; Wang, Y. F. Sesquilignans and sesquiterpenoid from the stem barks of Illicium simonsii and their anti-AChE activity. *Nat. Prod. Bioprospect*. **2012**, *2*, 133-137.

(15) Wang, W.; Fu, X. W.; Dai, X. L.; Hua, F.; Chu, G. X.; Chu, M. J.; Hu, F. Lin.; Ling, T. J.; Gao, L. P.; Xie, Z. W.; Wan, X. C.; Bao, G. H. Novel acetylcholinesteraseinhibitors from Zijuan tea and biosynthetic pathway of caffeoylated catechin in tea plant. *Food. Chem*. **2017**, *237*, 1172-1178.

(16) Zhao, C. C.; Chen, J.; Shao, J. H.; Shen, J.; Li, K. H.; Gu, W. Y.; Li, S. H.; Fan, J. D. Neolignan constituents with potential beneficial effects in prevention of type 2

366 diabetes from viburnum fordiae hance fruits. *J. Agric. Food Chem*. **2018**, *66*,
367 10421-10430.
368 (17) Ellman, G. L.; Courtney, K. D.; Andres, V.; Feather, R. M. A new and rapid
369 colorimetric determination of acetylcholinesterase activity. *Biochem. Pharmacol*.
370 **1961**, 88-90.
371 (18) Takara, K.; Matsui, D.; Wada, K.; Ichiba, T.; Nakasone, Y. New antioxidative
372 phenolic glycosides isolated from *Kokuto* non-centrifuged cane sugar. *Biosci.*
373 *Biotechnol. Biochem*. **2002**, *66 (1)*, 29-35.
374 (19) Lyu, Q.; Kuo, T. H.; Sun, C. D.; Chen, K. S.; Hsu, C. C.; Li, X.
375 Comprehensive structural characterization of phenolics in litchi pulp using tandem
376 mass spectral molecular networking. *Food Chem.* **2019**, *282*, 9-17.
377 (20) Braga, A. C. H.; Zacchino, S.; Héctor, B.; Manuel, G. S.; Edmundo, A. R. ^{13}C
378 NMR spectral and conformational analysis of 8-*O*-4′ neolignans. *Phytochemistry*.
379 **1984**, *23(9)*, 2025-2028.
380 (21) Noriko, M.; Masao, K. Studies on the costituents of Lonicera species.X.
381 Neolignan glycosides from the leaves of Lonicera gracilipes var. glandulosa Maxim.
382 *Chem. Pharm. Bull*. **1996**, *44(9)*, 1676-1679.
383 (22) Lu, Y. Y.; Xue, Y. B.; Liu, J. J.; Yao, G. M.; Li, D. Y.; Sun, B.; Zhang, J. W.;
384 Liu, Y. F.; Qi, C. X.; Xiang, M.; Luo, Z. W.; Du, G.; Zhang, Y. H.
385 (±)-Acortatarinowins A−F, norlignan, neolignan, and lignan enantiomers from
386 *Acorus tatarinowii*. *J. Nat. Prod*. **2015**, *78*, 2205-2214.
387 (23) Hua, F.; Zhou, P.; Wu, H. Y.; Chu, G. X.; Xie, Z. W.; Bao, G. H. Inhibition of

388 flavonoid glycosides from Lu'an GuaPian tea on α-glucosidase and α-amylase:
389 molecular docking and interaction mechanism. *Food. Funct*. **2018**, *9*, 4173-4183.
390 (24) Cheng, J.; Wu, F. H.; Wang, P.; Ke, J. P.; Wan, X. C.; Qiu, M. H.; Bao, G. H.,
391 Flavoalkaloids with a pyrrolidinone ring from Chinese ancient cultivated tea Xi-Gui. *J.*
392 *Agric. Food Chem.* **2018**, *66*, 7948-7957.
393 (25) Li, X.; Liu, G. J.; Zhang, W.; Zhou, Y. L.; Ling, T. J.; Wan, X. C.; Bao, G. H.
394 Novel flavoalkaloids from white tea with inhibitory activity against formation of
395 advanced glycation end products. *J. Agric. Food Chem*. **2018**, *66*, 4621-4629.
396 (26) Wang, W.; Zhu, B. Y.; Wang, P.; Zhang, P.; Deng, W. W.; Wu, F. H.; Ho, C. T.;
397 Ling, T. J.; Zhang, Z. Z.; Wan, X. C; Bao, G. H. Enantiomeric trimethylallantoin
398 monomers, dimers, and trimethyltriuret: Evidence for an alternative catabolic pathway
399 of caffeine in tea plant. *Org. Lett*. **2019**, *21*, 2672-2675.
400 (27) Quinn, R. A.; Nothias, L. F.; Vining, O.; Meehan, M.; Esquenazi, E.; Dorrestein,
401 P. C. Molecular networking as a drug discovery, drug metabolism, and precision
402 medicine strategy. *Trends. Pharmacol. Sci*. **2017**, *38(2)*, 143-154.
403 (28) Ge, Y. W.; Zhu, S.; Yoshimatsu, K.; Komatsu, K. MS/MS similarity networking
404 accelerated target profiling of triterpene saponins in Eleutherococcus senticosus
405 leaves. *Food Chem.* **2017**, *227*, 444-452.
406 (29) Şöhretoğlu, D.; Sari, S.; Barut, B.; Özel, A. Tyrosinase inhibition by a rare
407 neolignan: Inhibition kinetics and mechanistic insights through in vitro and in silico
408 studies. *Comput. Biol. Chem*. **2018**, *76*, 61-66.
409 (30) Zhao, P.; Zhang, H.; Han, F. Y.; Guo, R.; Huang, S. W.; Lin, B.; Huang, X. X.;

410 Song, S. J. Chiral resolution and neuroprotective activities of enantiomeric 8-*O*-4′
411 neolignans from the fruits of *Crataegus pinnatifida* Bge. *Fitoterapia*. **2019**, *136*,
412 104164.
413 (31) Sun, S. W.; Liu, Y.; Liu, X. H.; Zhang, S.; Wang, W.; Wang, R. R.; Hou, Y. X.;
414 Wang, W. Neolignan glycosides from Spiraea salicifolia and their inhibitory activity
415 on pro-inflammatory cytokine interleukin-6 production inlipopolysaccharide
416 -stimulated RAW 264.7 cells. *Nat. Prod. Res*. **2018**, 1478-6419.

417 **Figure Captions**

418 **Figure 1.** The structures of compounds **1-16** from Huangjinya green tea. Rha,
419 rhamnose unit; Glc, Glucose unit.

420 **Figure 2.** Clusters based molecular network of neolignan glycosides (I) and catechins
421 (III) in Huangjinya green tea extracts detected by the UPLC-Q-TOF-MS/MS (The
422 picture in black frame is the complete molecular networking of HGTE, which shows a
423 global overview of the spectral similarity of all MS^2 spectra from this dataset.
424 Numbered amplified regions in the global network are shown. The nodes with color
425 represent the discriminating features of the project, which is at the upper right of the
426 figure. The arrows are showing the corresponding relationship between the structure
427 of compounds and the nodes in the network one by one.).

428 **Figure 3.** A: The molecular networking of flavonoid glycosides (II) in Huangjinya
429 green tea extracted from **Figure 2** (Lables as green were compounds identified
430 through GNPS library and MS^2 spectra (B)). B: MS^2 spectra of relative compounds.
431 Rha, rhamnose unit; Glc, Glucose unit.

432 **Figure 4.** Selected two dimentioanl nuclear magnetic resonance correlations (2D
433 NMR) including the key 1H 1H COSY (heavy solid line), HMBC (solid single
434 arrowhead line), and ROESY (compound **1**) or NOESY (dashed double arrowhead
435 line) correlations of compound **2**.

437 **Table 1.** ^{1}H and ^{13}C NMR Data of Compounds **1** and **2**.

No.	**1**[a]		**1a**[b]	**2**[a]		**2a**[b]
	δ_C	δ_H (J, Hz)	δ_H (J, Hz)	δ_C	δ_H (J, Hz)	δ_H (J, Hz)
1	133.2			130.3		
2	112.3	6.99 (s)	6.97 (d, 1.2)	112.3	6.98 (s)	6.98 (d, 1.8)
3	147.4			147.3		
4	146.0			146.1		
5	115.1	6.66 (d, 7.8)	6.87 (d, 7.8)	115.0	6.66 (d, 7.8)	6.90 (d, 7.8)
6	120.1	6.78 (d, 7.8)	6.82 (dd, 8.4, 1.8)	120.2	6.79 (d, 7.8)	6.93 (dd, 8.4, 1.8)
7	72.0	4.76 (dd, 4.2, 4.8)	4.97 (dd, 3.0, 4.2)	78.3	4.93 (d, 4.2)	4.96 (d, 8.4)
8	82.2	4.44 (m)	4.11 (m)	82.6	4.39 (m)	3.97 (m)
9	68.3	3.48 (dd, 11.4, 5.4)	3.45 (d, 1.2)	60.3	3.18 (dd, 10.8, 4.2)	3.48 (d)[c]
		3.95 (m)	3.65 (m)		3.65 (m)	3.62 (m)
—OMe	55.9	3.72 (s)	3.89 (s)	55.9	3.71 (s)	3.90 (s)
1′	135.7			135.8		
2′	113.4	6.73 (s)	6.77 (d, 1.2)	113.2	6.78 (s)	6.79 (d, 1.8)
3′	149.9			149.9		
4′	146.2			146.2		
5′	116.7	6.95 (d, 7.8)	6.89 (d, 7.8)	116.3	6.93 (d, 7.8)	7.03 (d, 7.8)
6′	120.6	6.62 (d, 7.8)	6.75 (dd, 7.8, 1.2)	120.5	6.62 (d, 7.8)	6.76 (dd, 7.8, 1.8)
7′	31.7	2.48 (t, 1.8)	2.69 (t-like, 7.8)	31.7	2.48 (t-like, 8.4)	2.69 (t-like, 9.0)
8′	34.9	1.67 (m)	1.89 (m)	34.9	1.67 (m)	1.89 (m)
9′	60.6	3.37 (t, 5.4)	3.69 (t, 6.0)	60.6	3.39 (t, 6.0)	3.69 (t, 6.0)
—OMe	56.1	3.68 (s)	3.90 (s)	56.0	3.74 (s)	3.91(s)
1″	103.7	4.08 (d, 7.8)		102.7	4.39 (d, 7.8)	
2″	73.9	2.95 (m)		74.7	3.02 (m)	
3″	77.1	3.10 (m)		77.1	3.13 (m)	
4″	70.4	3.01 (m)		70.7	3.02 (m)	
5″	77.3	3.01 (m)		77.5	3.02 (m)	
6″	61.4	3.37 (m), 3.61 (m)		61.4	3.39 (m), 3.57 (m)	
4-OH		8.75s		4-OH	8.78s	
7-OH		5.25 (d, 4.8)		9-OH	4.62 (t, 5.4)	
2″-OH		4.96 (d, 4.8)		2″-OH	4.91 (d, 4.2)	
3″-OH		4.91 (d, 4.8)		3″-OH	4.90 (d, 4.2)	
4″-OH		4.86 (d, 3.6)		4″-OH	4.86 (d, 4.2)	
6″-OH		4.48 (t, 6.0)		6″-OH	4.28 (t, 5.4)	
9′-OH		4.42 (m)		9′-OH	3.33 (m)	

438 [a]^{1}H at 600 MHz and ^{13}C NMR at 150 MHz in DMSO-d_6. [b]^{1}H at 600 MHz in $CDCl_3$.

439 [c]Overlapped with other signals. s, single peak; d, double peaks; m, multipeaks.

441 **Figure 1**.

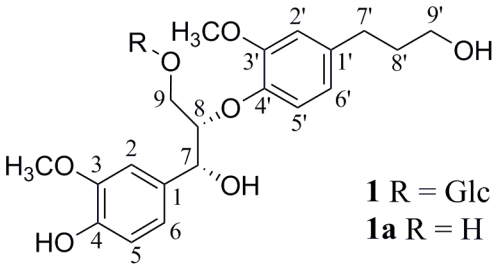

1 R = Glc
1a R = H

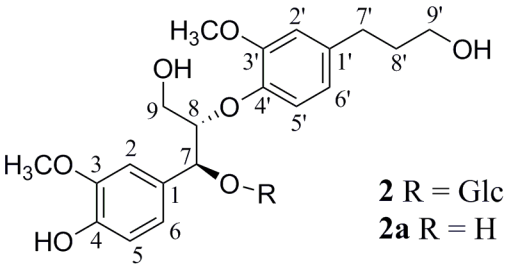

2 R = Glc
2a R = H

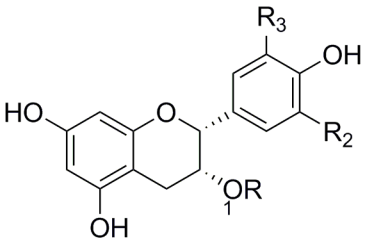

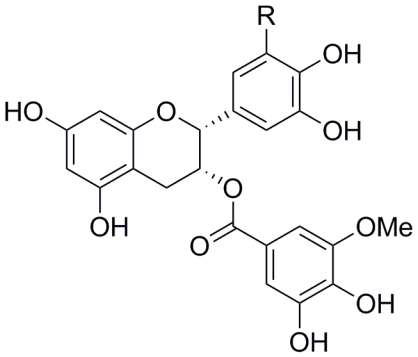

3 $R_1 = R_2 = H$, $R_3 = OH$ (EC)
4 $R_1 = H$, $R_2 = R_3 = OH$, (EGC)
5 $R_1 = G$, $R_2 = H$, $R_3 = OH$ (ECG)
6 $R_1 = G$, $R_2 = R_3 = OH$ (EGCG)
7 $R_1 = G$, $R_2 = R_3 = H$ (EAG)

8 R = H (ECG3"Me)
9 R = OH (EGCG3"Me)

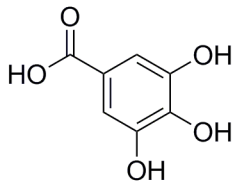

10

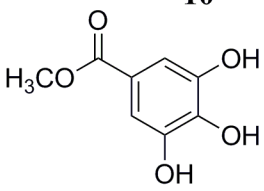

11

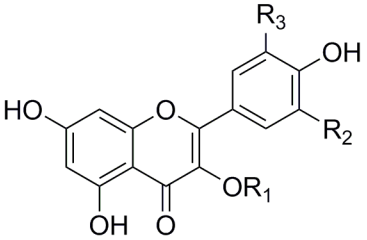

12 $R_1 = R_2 = R_3 = H$
13 $R_1 = R_2 = H$, $R_3 = OH$
14 $R_1 = H$, $R_2 = R_3 = OH$
15 R_1 =Rha (1➝6) Glc, $R_2 = R_3 = H$
16 R_1 =Rha (1➝6) Glc, $R_2 = H$, $R_3 = OH$

442

444 **Figure 2**.

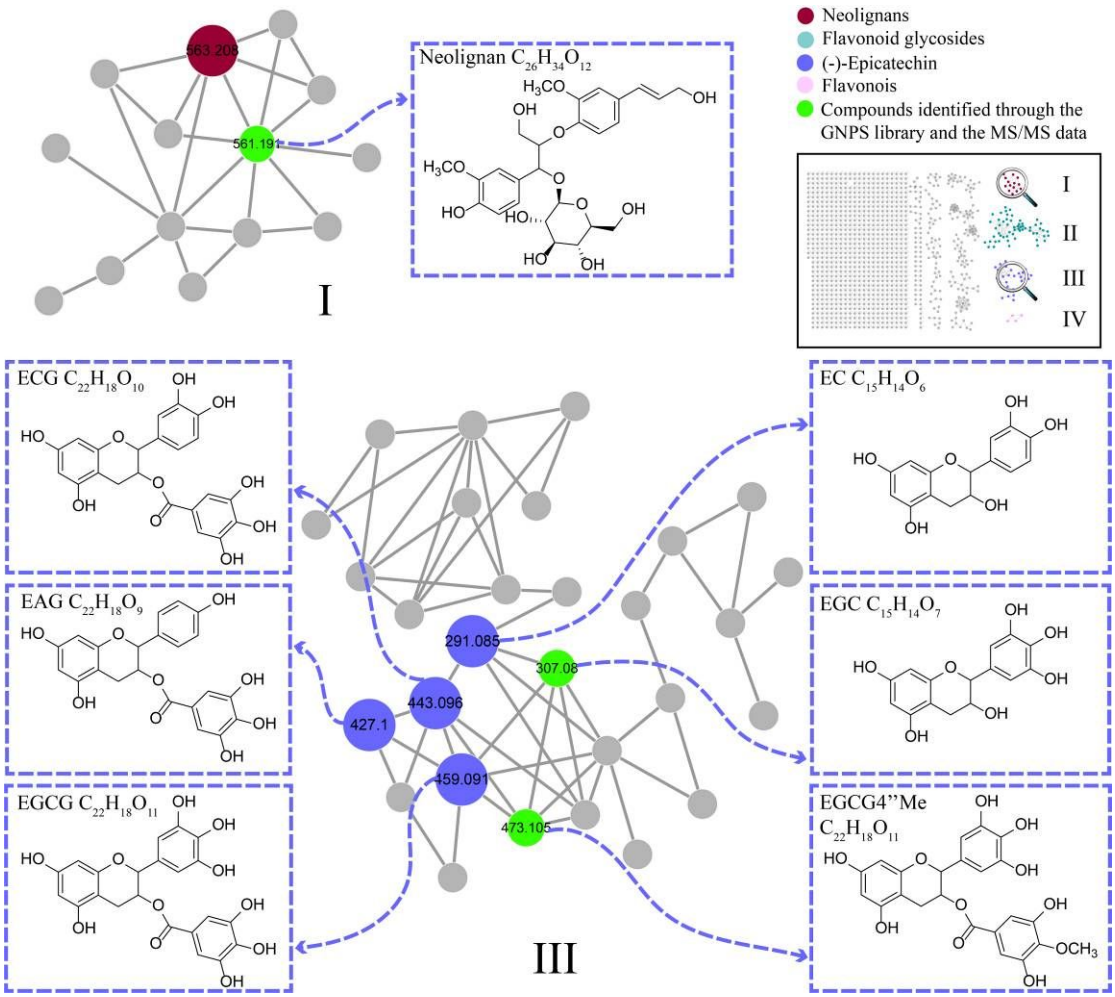

445

447 **Figure 3**.

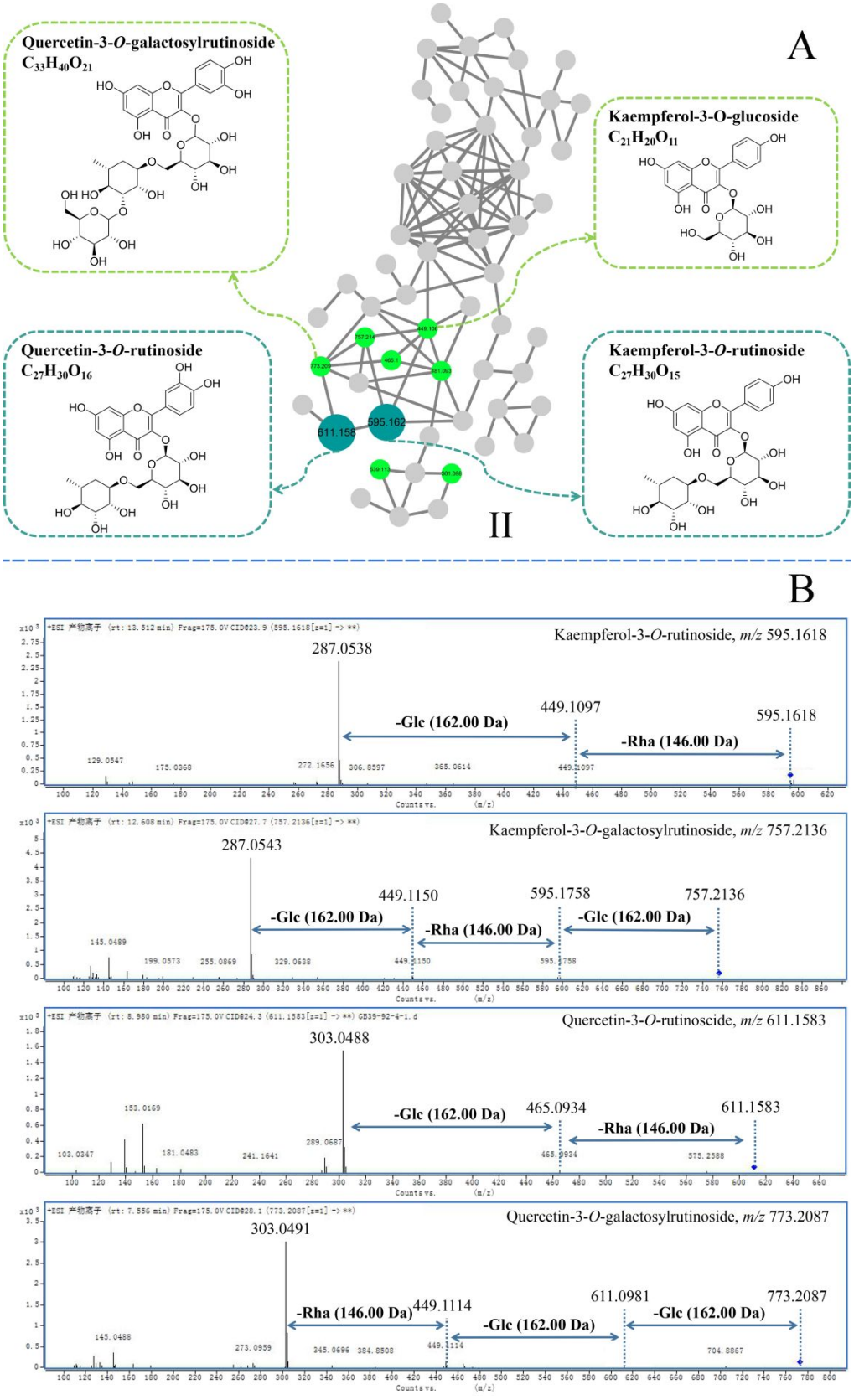

448

450 **Figure 4**.

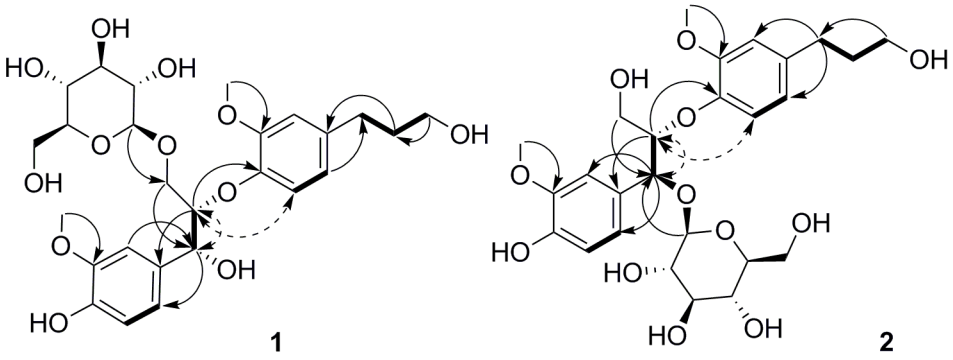

451

453 **TOC**

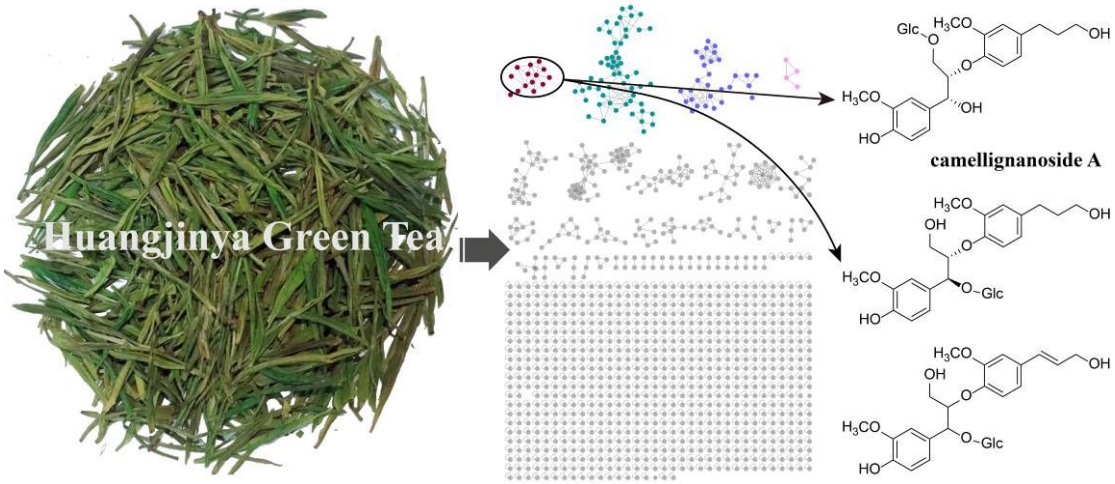

454